HIGH TEMPERATURE TENSILE AND TRIBOLOGICAL PROPERTIES

5.1 Introduction

In many tribological applications counteracting parts undergo sufficiently high temperature; therefore, it becomes important to have knowledge of relevant properties at high temperature. In the present chapter, to check high temperatures suitability and performance of AA5052/ZrB_2 composites tensile and wear test were conducted at different temperatures.

In this chapter the effect of temperature on tensile properties of selected compositions has been evaluated and discussed. Wear and friction properties have also been studied for selected compositions. Tensile and wear properties have been evaluated at 50°, 100°, 150° and 200°C. The high temperature properties have been compared with ambient temperature properties for same operating conditions. Tensile fractured surface and worn surface are examined under SEM and EDS to understand the mode of failure and wear mechanism involved during the process at high temperature. Worn surfaces are also studied under profilometer for their 2D, 3D surface topography and surface roughness.

5.2 Tensile Properties

Tensile tests for composites were conducted at an interval of 50°C up to a temperature of 200°C at a strain rate of $1.07 \times 10^{-3}\ s^{-1}$. Figure 5.1a-c shows the variation of UTS, YS and percentage elongation with temperature for 6 and 9 vol. % ZrB_2 composites.

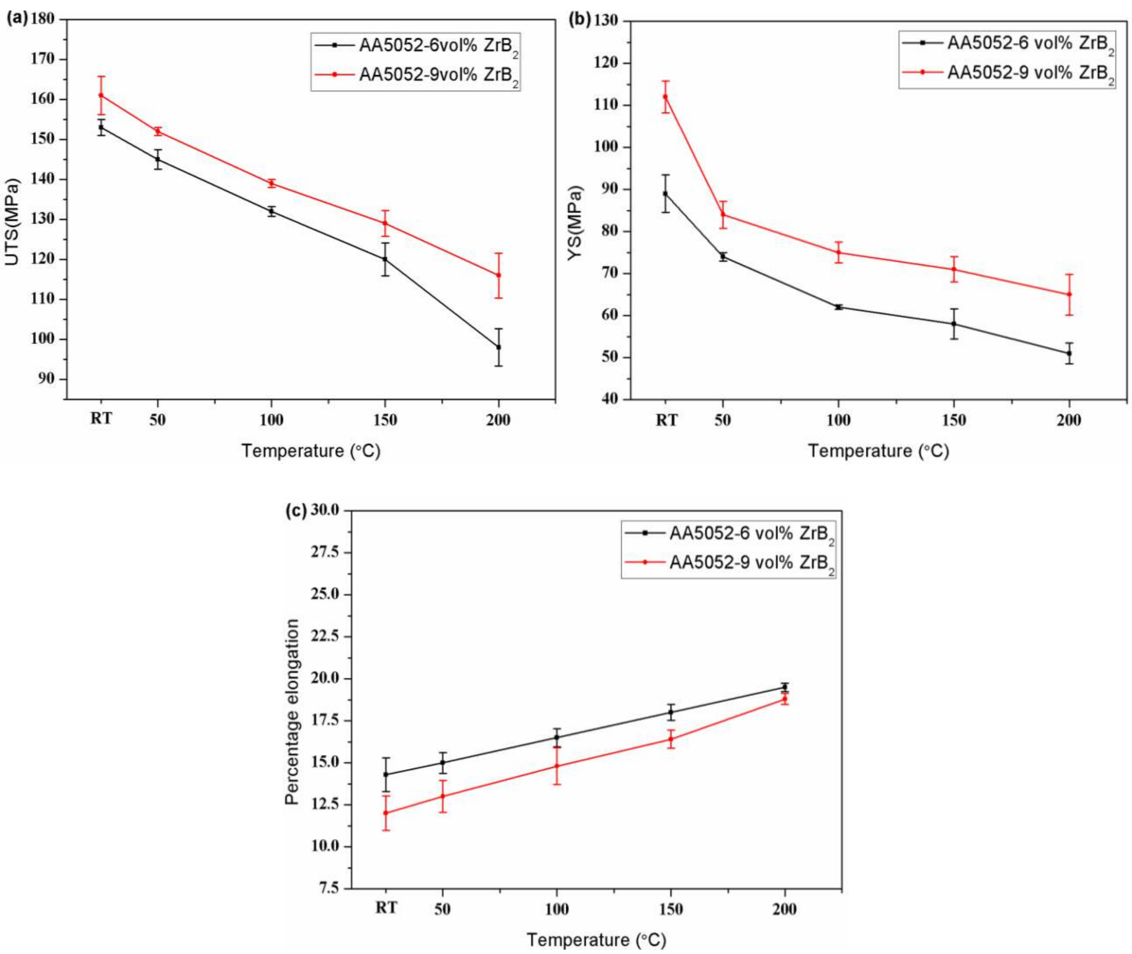

Figure 5.1 - Variation of (a) UTS (b) YS and (c) percentage elongation with temperature

The Experimental results reveal that UTS and YS of both the composites decrease linearly with increase in operating temperature. However, AA5052 - 9 vol. % ZrB_2 composite exhibits good resistance to high temperature effects in terms of strength. Even at 150°C the UTS of the 9 vol. % ZrB_2 composite is 81% of the ambient temperature strength, and at 200°C also 72% of the ambient temperature strength is retained. It should also be noted that percentage elongation (ductility) increases as the test temperature increases for both the composites due to thermal softening of the matrix. AA5052 - 9 vol. % ZrB_2 composite shows lesser improvement in elongation due to its high strength and less thermal softening as compared to AA5052 - 6 vol. % ZrB_2 composite.

5.3 Fractography

Fractured surface of composite with 9 vol. % ZrB_2 particles are shown in SEM micrographs (Fig. 5.2a-d). These figures correspond to tests conducted at RT, 100°, 150° and 200°C. The fractured surface morphology at high temperature is quite different from that of the room temperature. At room temperature the fractured surface clearly shows a large crack, initiated by high stresses due to the presence of large clusters of hard ZrB_2 particles as shown in Fig.5.2a. The major form of fracture, at room temperature, is the rupture of ZrB_2 particles from the matrix. Small size dimples are also seen on the surface. With rise in temperature large size dimples of the matrix material along with large voids are seen on the surface. When the temperature reaches to 200°C (Fig.5.2d), thermal softening takes place and voids in the matrix act as dominant fracture mode, thereby ductility is increased [Han et al., 2015;Yi et al., 2006a].

5.4 Wear and Friction

The increasing use of PAMCs in high temperature applications has compelled engineers and scientists to study high-temperature tribology of these materials. Variety of components are subjected to the wear problem at high temperature, such as wear of cutting tools in dry machining, die wear in hot extrusion and drawing operation, seal rings, valve seats, and bearing parts [Kumar et al., 2016b].

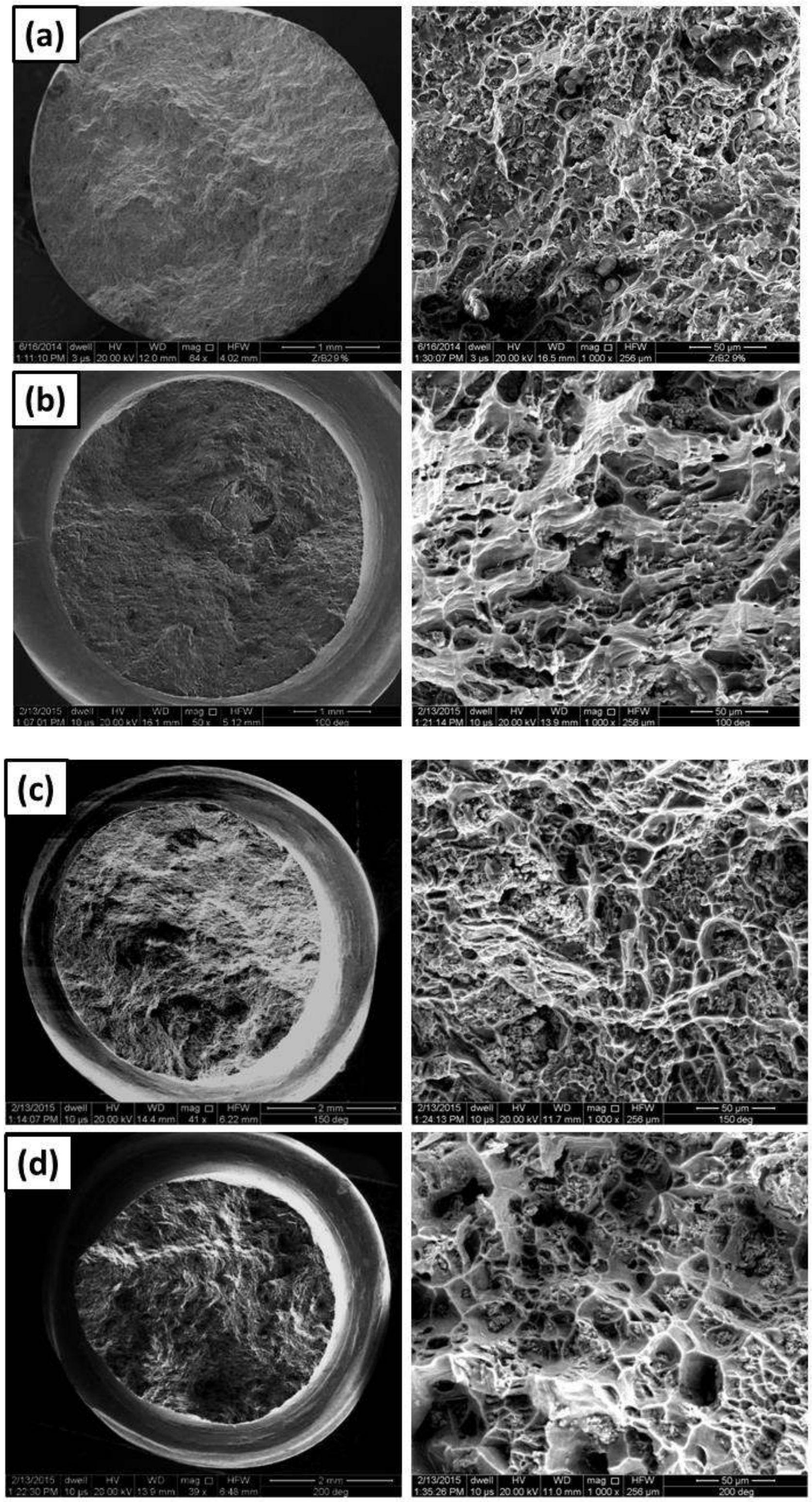

Figure 5.2 - Fractographs of composite with 9 vol. % ZrB_2 at different temperatures (a) RT (b) 100°C (c) 150°C and (d) 200°C

Other examples include high speed rotating or reciprocating mass items such as pistons, drive shafts, cylinder bores or liners and brake rotors. These components often operate at temperatures approaching 0.4–0.8 of the melting point of aluminum matrix alloy, which could lead to seizure during operation if oil deficiency or adverse operating conditions arise. Therefore, wear and friction behaviour of these components at high temperature must be taken into consideration in the component design aspect [Kumar et al., 2016b].

5.4.1 Effect of vol. % of ZrB_2 Particles

Figure 5.3a-d shows the effect of ZrB_2 vol. % on wear rate at different loads (10 - 40 N), but for same sliding velocity 0.5 m/s and sliding distance 1000 m. It is observed from figure that for a specific temperature wear rate decreases as a function of vol. % of ZrB_2. The lower wear rate at high vol. % of ZrB_2 particles is attributed to the grain refinement and enhanced hardness & strength in composites resulting from increased dislocation density. Moreover, local strain fields are generated around ZrB_2 particles during solidification due to difference in coefficient of thermal expansion of ZrB_2 particle and aluminium alloy matrix. These strain fields resist the crack propagation and subsequently material removal during sliding motion. Clear interface and good interfacial bonding between particles and matrix also contribute to lower wear rates [Rajan et al., 2014]. The increased ZrB_2 amount in mechanically mixed layer (MML) also restricts the removal of material from the surface due to increased hardness of composite also causing the wear rate to decrease. This is in agreement with Archard's wear law [Archard, 1953]. Further, it is also observed from Fig. 5.3 that as the temperature increases role of abrasive particles increases. Even at high temperature i.e. 200°C increase in wear rate is much less in case of composite with 9 vol. % ZrB_2 as compared to base alloy and this phenomenon is more pronounced in case of normalised wear rate. On the contrary, an increase in coefficient of friction is observed with increase in vol. % of hard ZrB_2 particles (Fig. 5.4 a-d). With an increase in vol. % of ZrB_2 particles in the MML total coefficient of friction increases as a result of increased presence of large abrasive particles. Whereas, other factors contributing to friction remain more or less same, and a continuous increase in coefficient of friction is observed [Kumar et al., 2016b].

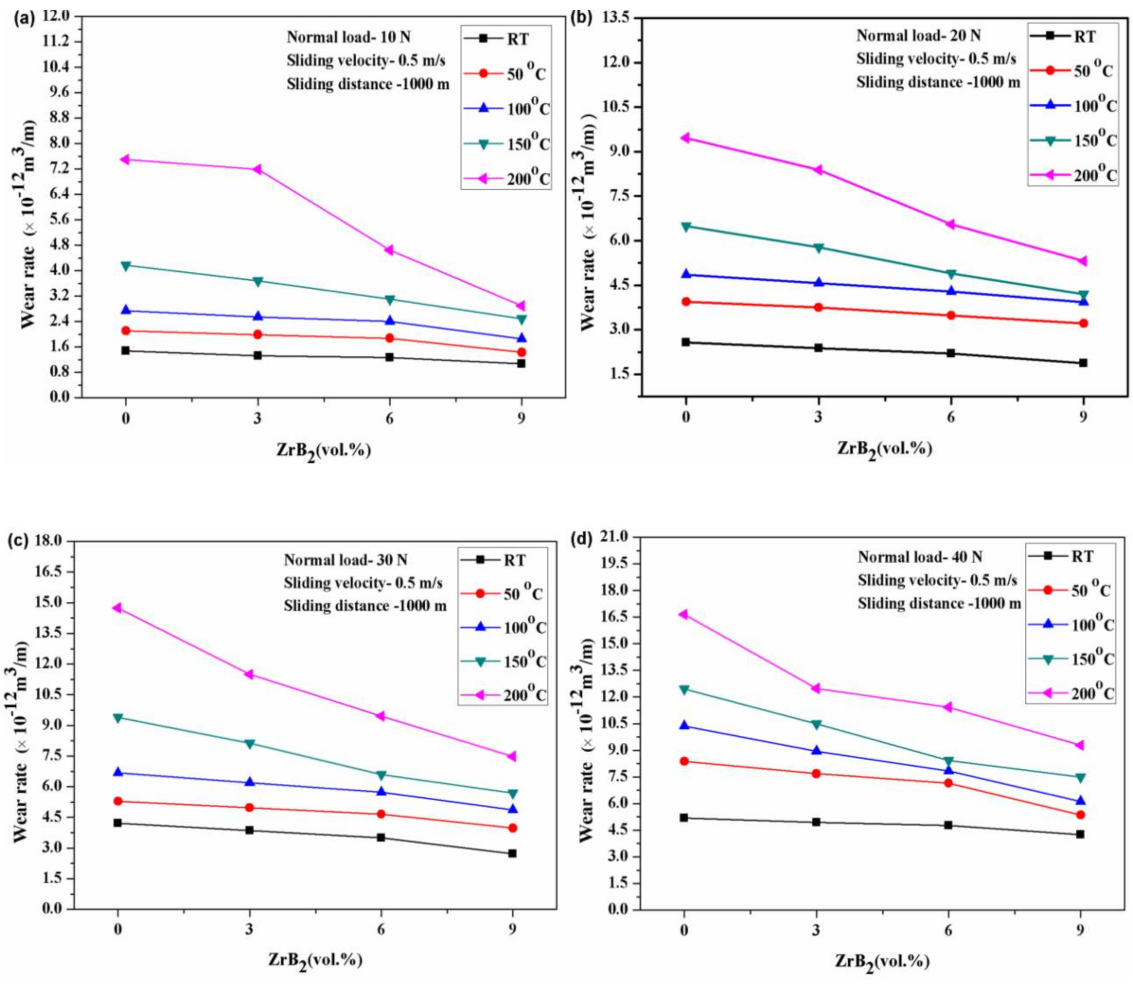

Figure 5.3 - Variation of wear rate with ZrB_2 vol. % at (a) 10 N (b) 20 N (c) 30 N and (d) 40 N load for different temperatures [Kumar et al., 2016b]

Worn surfaces of base alloy and different composites tested at room temperature under 20 N load and 0.5 m/s sliding velocity were examined under SEM and morphology is shown in Fig.5.5a-d. Worn surfaces reveal distinct pattern of parallel grooves and ridges. The wear mode seems to be abrasive at room temperature. The surface exhibits deep grooves, cracks, high delamination and damaged area (Fig.5.5a). However, worn surface of composites reveal much shallow grooves, and less delamination due to the presence of ZrB_2 particles. The depth of grooves, delamination and damaged area are observed to reduce with increase in ZrB_2 amount (Fig. 5.5b-d). Moreover, cracks are not observed on the wear surfaces of composites [Kumar et al., 2016b].

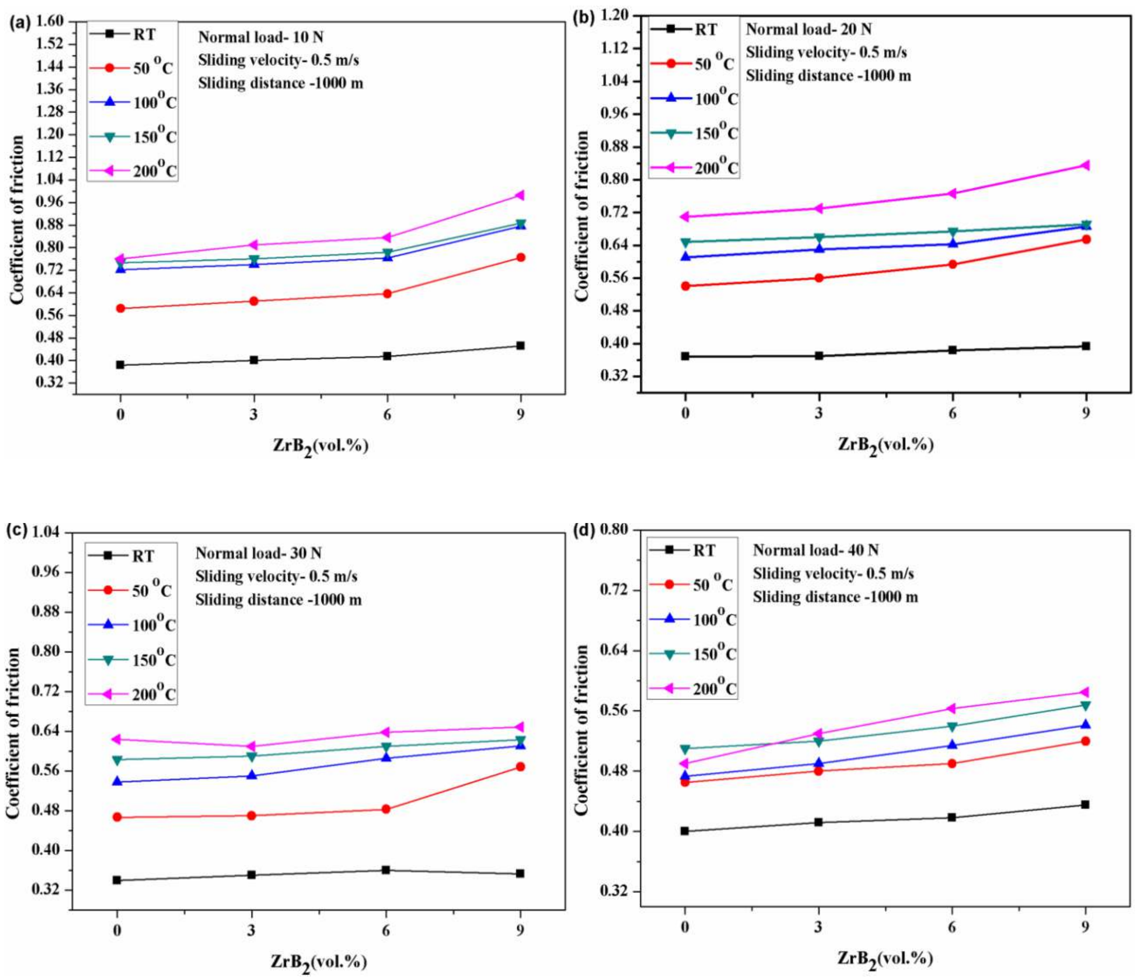

Figure 5.4 - Variation of COF with ZrB_2 vol. % at (a) 10 N (b) 20 N (c) 30 N and (d) 40 N load for different temperatures [Kumar et al., 2016b]

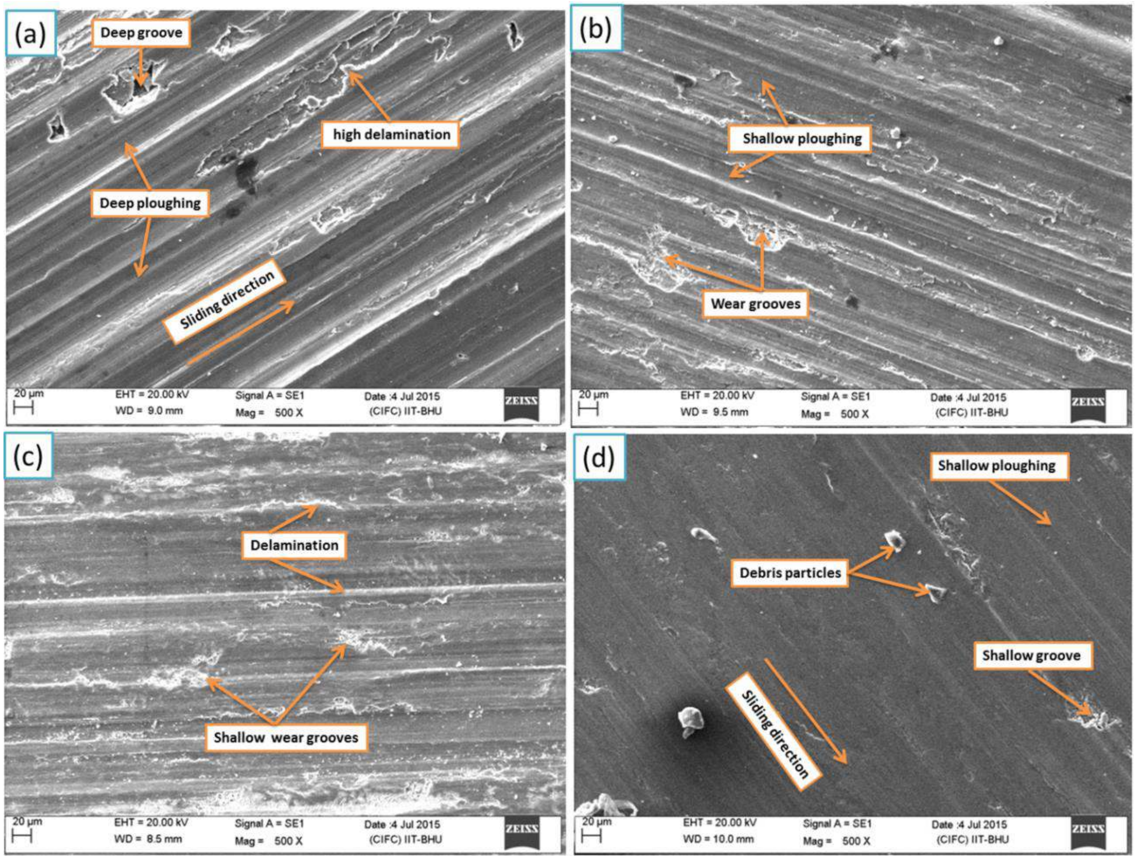

Figure 5.5 - Worn surface morphology of (a) base alloy (b) 3 vol. % ZrB_2 (c) 6 vol. % ZrB_2 and (d) 9 vol. % ZrB_2 composite at room temperature, 20 N load and 0.5 m/s sliding velocity [Kumar et al., 2016b]

Worn surface morphology at 200°C is shown in Fig. 5.6a-d. Worn surface reveal flakes, severe delamination of surface and large amount of metal flow during sliding at high temperature which leads to higher wear rate. Wear mode seems to be severe-metallic at high temperature. As observed from Fig. 5.6a, worn surface of base alloy exhibits severely damaged area and heavy metal flow, however, metal flow and deformation reduces with increase in the ZrB_2 vol. % in composites (Fig.5.6b-d). Worn surface morphology at 200°C has also been examined by 3D profilometer (Fig.5.7a-b) which reveals that composite's worn surface has relatively less roughness as compared to base alloy which is in agreement with the results [Kumar et al., 2016b].

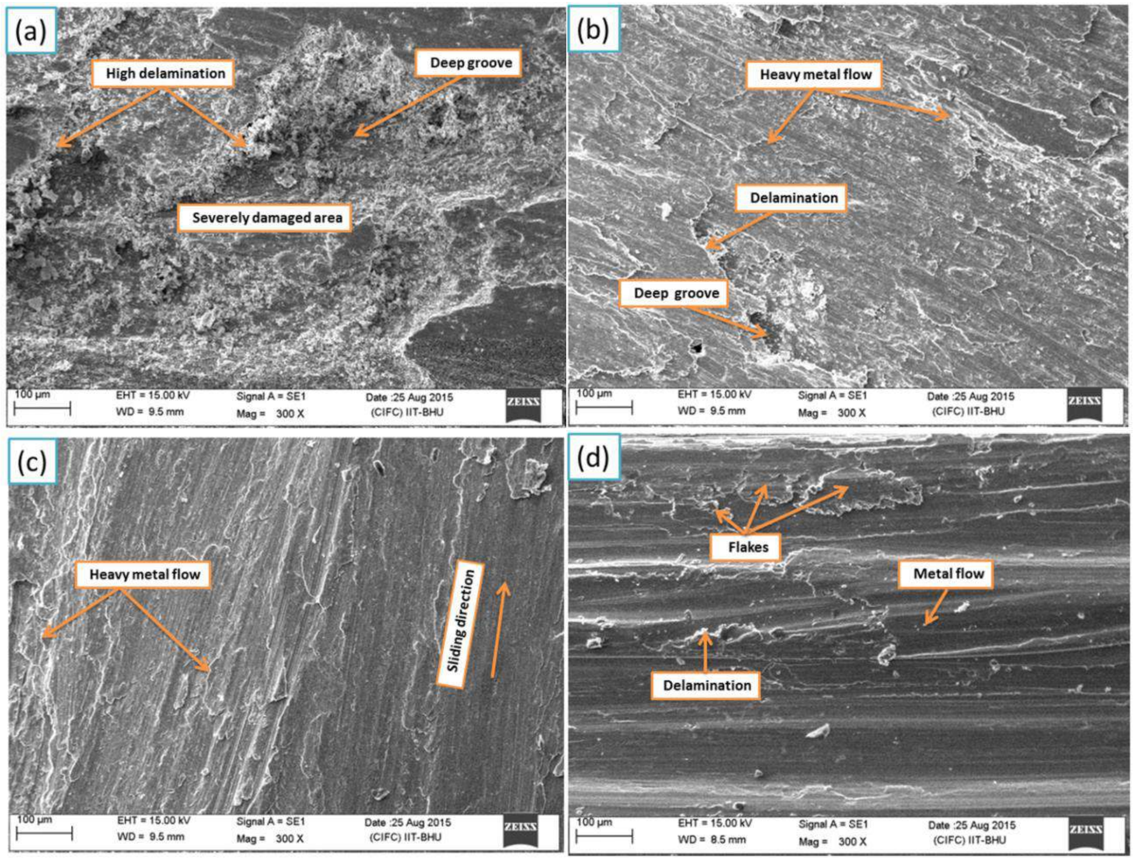

Figure 5.6 - Worn surface morphology of (a) base alloy (b) 3 vol. % ZrB_2 (c) 6 vol. % ZrB_2 and (d) 9 vol. % ZrB_2 composite at 200°C temperature, 20 N load and 0.5 m/s sliding velocity [Kumar et al., 2016b]

5.4.2 Effect of Temperature

Figures 5.8 and 5.9 show the effect of temperature on wear rate and coefficient of friction of composites at different loads from 10 to 40 N. It is observed from Fig. 5.8a-d that for a constant vol. % of ZrB_2 particles wear rate increases as a function of temperature. Aluminium matrix gets softened with increase in the temperature which leads to more penetration of hard asperities into soft matrix causing more material removal and giving rise to enhanced wear rate. Wear rate of base alloy increases slowly and wear mode changes from mild-oxidative to severe-metallic at transition temperature of 100°C, beyond this temperature wear rate increases sharply with increase in temperature.

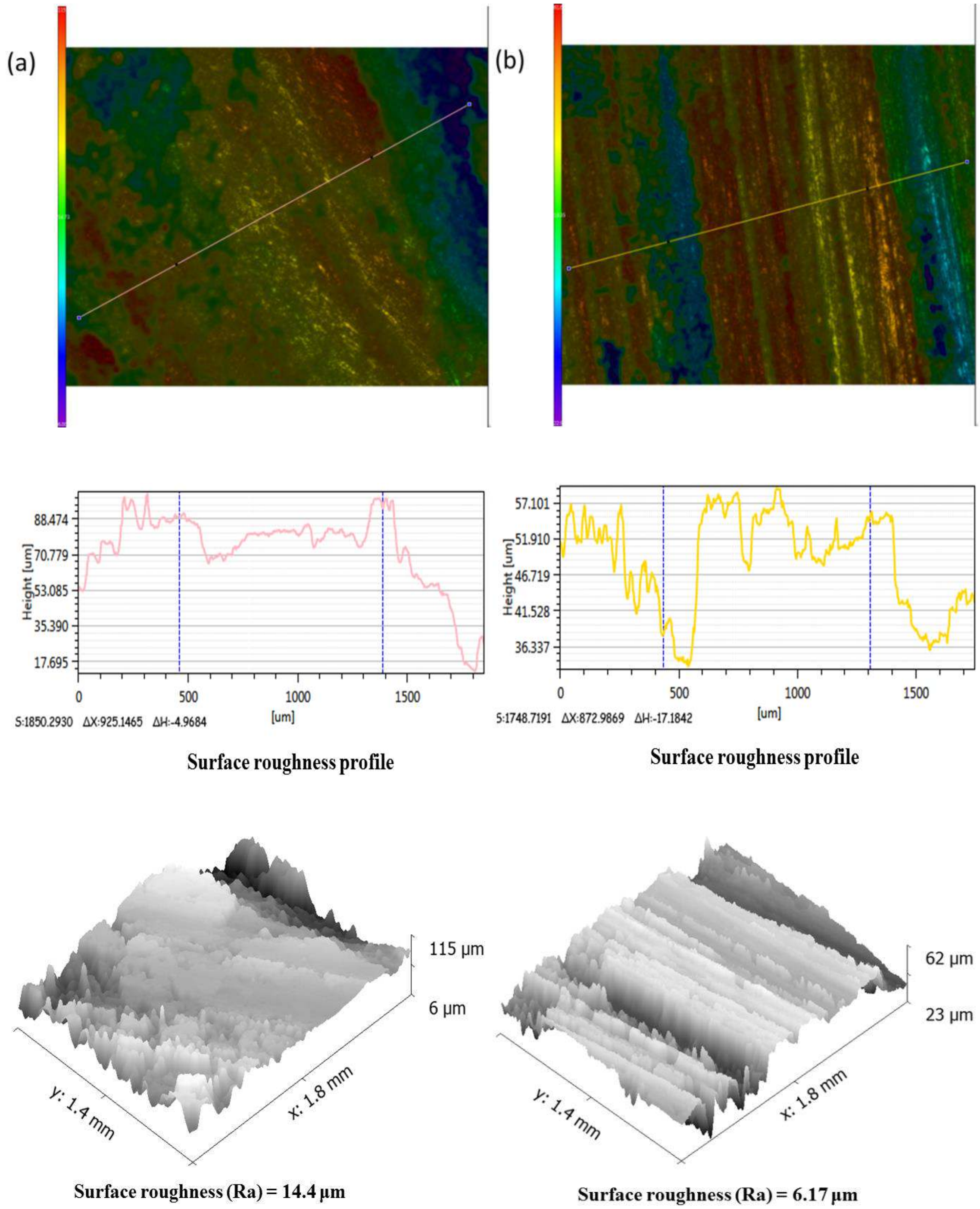

Figure 5.7 - 2D and 3D topography of worn surface of (a) base alloy, and (b) 9 vol. % ZrB_2 composite at 200°C temperature, 20 N load and 0.5 m/s sliding velocity under profilometer [Kumar et al., 2016b]

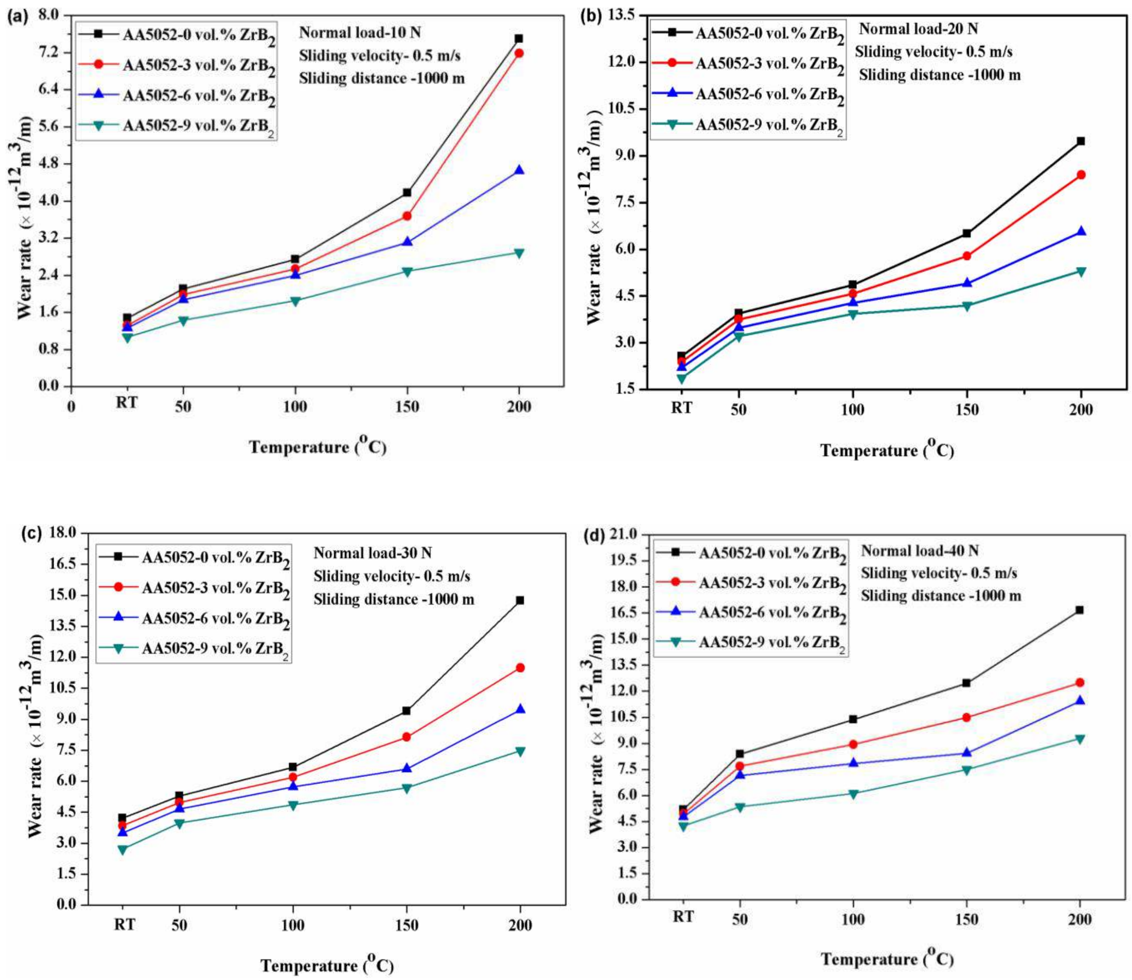

Figure 5.8 - Variation of wear rate with different temperatures at (a) 10 N (b) 20 N (c) 30 N and (d) 40 N load for different composites [Kumar et al., 2016b]

However, a shift in transition temperature from mild-oxidative to severe-metallic is observed and it reaches to 150°C in case of composite with 9 vol. % ZrB_2. Increase in transition temperature may be attributed to the better dimensional stability of matrix due to increased amount of reinforcement particles in composites. It has also been observed by other workers who worked with different reinforcements [Kumar et al., 2009; 2010b; Rajan et al., 2014; Singh and Alpas, 1995]. EDS spectrum of worn surface of alloy tested at 50°C is shown in Fig. 5.10 which consists of aluminium and oxygen peaks confirming the formation of oxidative layer on the worn surface, and the wear mode is oxidative. Absence of iron peaks indicates that wear of steel disk has not taken place at all [Kumar et al., 2016b].

Coefficient of friction also increases with increase in temperature for all compositions at different loads (Fig. 5.9a-d). This improvement may be attributed to the increased adherence between the disc and pin sample at higher temperature [Zhu et al., 2012]. Further, large oxide formation and generation of cracks in oxide layer also contributes to high coefficient of friction and wear [Kumar et al., 2016b].

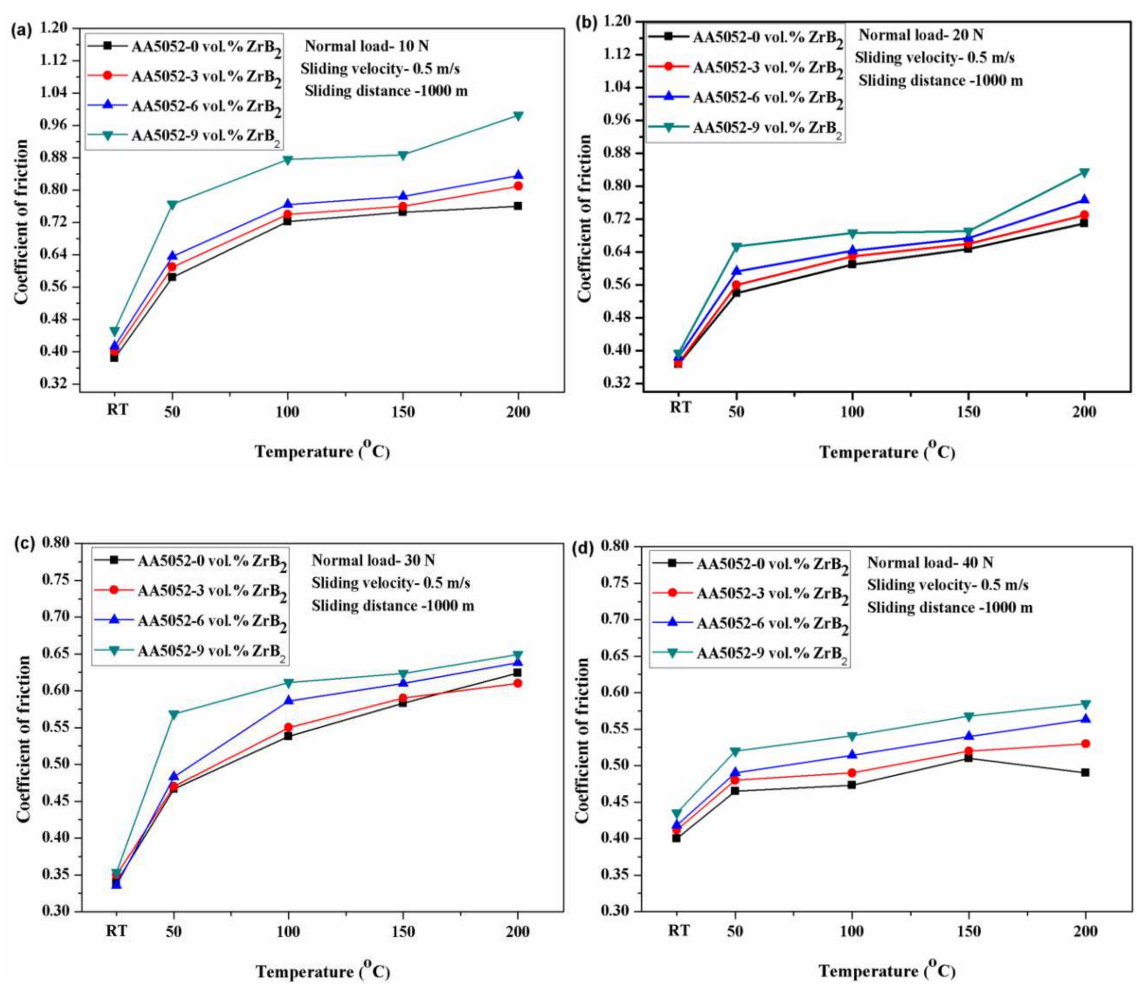

Figure 5.9 - Variation of COF with temperature at (a) 10 N (b) 20 N (c) 30 N and (d) 40 N load for different composites [Kumar et al., 2016b]

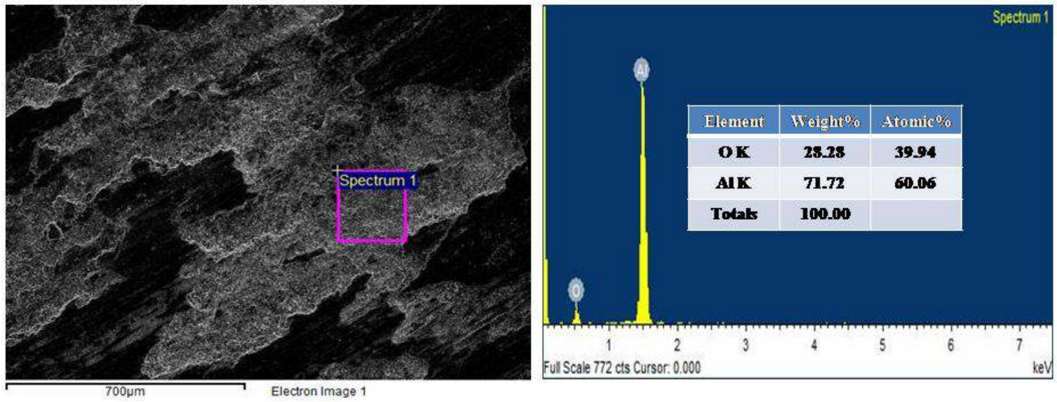

Figure 5.10 - EDS spectrum of worn surface of alloy tested at 50°C showing oxidative wear mode [Kumar et al., 2016b]

Worn surface morphology of AA5052 - 6 vol. % ZrB_2 composite at various temperatures ranging from room temperature (RT) to 200°C is shown in Fig. 5.11a-e. Worn surface reveals the ploughing, parallel grooves and ridges at room temperature (Fig. 5.11a), whereas, craters formation takes place at high temperature due to thermal softening of matrix. Worn surface area gets covered with large craters with increase in temperature up to 150°C (Fig. 5.11b-d), and beyond that temperature high delamination and metal flow occur during sliding which is indicative of severe-metallic wear leading to high wear rate (Fig. 5.11e). Wear debris analysis also shows the fine size debris particles along with small flakes at room temperature (Fig. 5.12a), and coarse size debris particles and large flakes are found at 200°C (Fig. 5.12b). 3D profilometry and surface roughness measurement of worn surfaces are also in agreement revealing increased surface roughness at 200°C as compared to room temperature (Fig. 5.13a-b) [Kumar et al., 2016b].

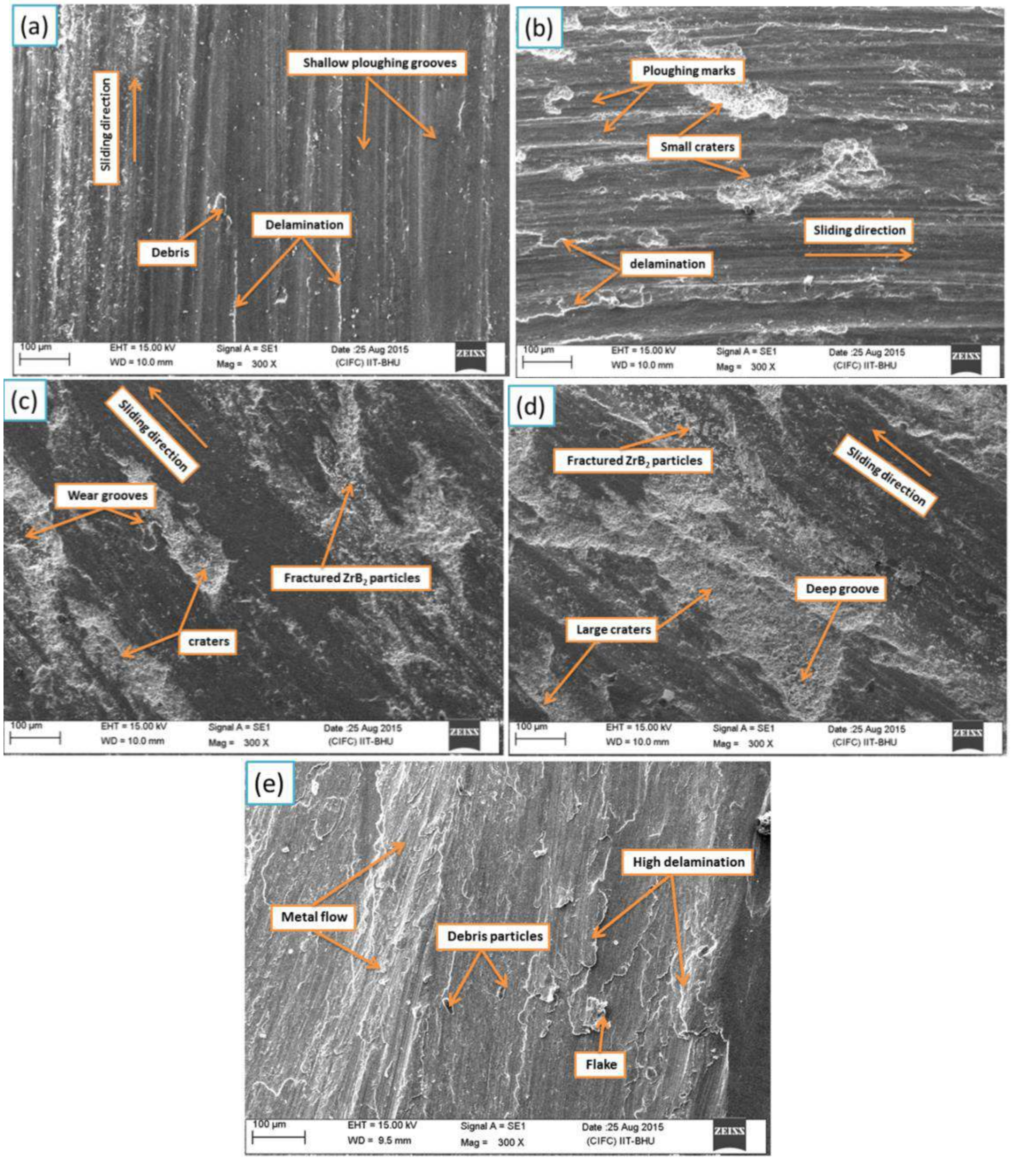

Figure 5.11 - Worn surface morphology of AA5052 - 6 vol. % ZrB_2 composite at (a) RT (b) 50°C (c) 100°C (d) 150°C, and (e) 200°C, at 20 N load and 0.5 m/s sliding velocity [Kumar et al., 2016b]

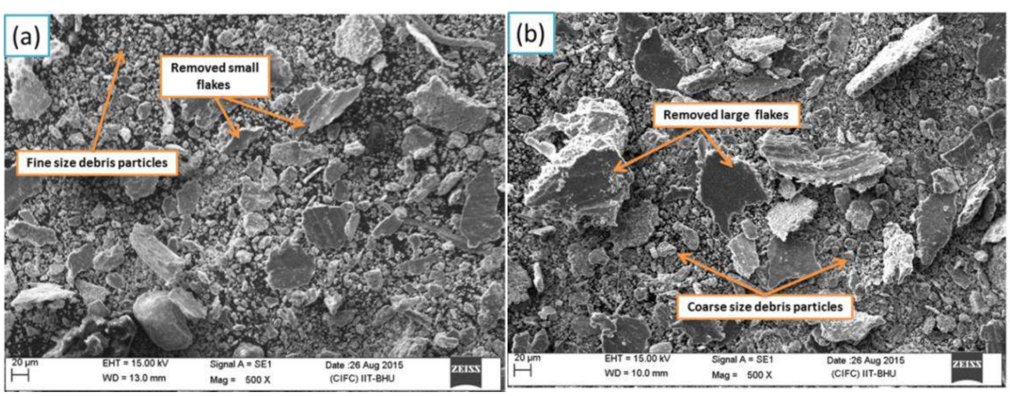

Figure 5.12 - Debris of composite with 6 vol. % ZrB_2 at (a) RT and (b) 200°C [Kumar et al., 2016b]

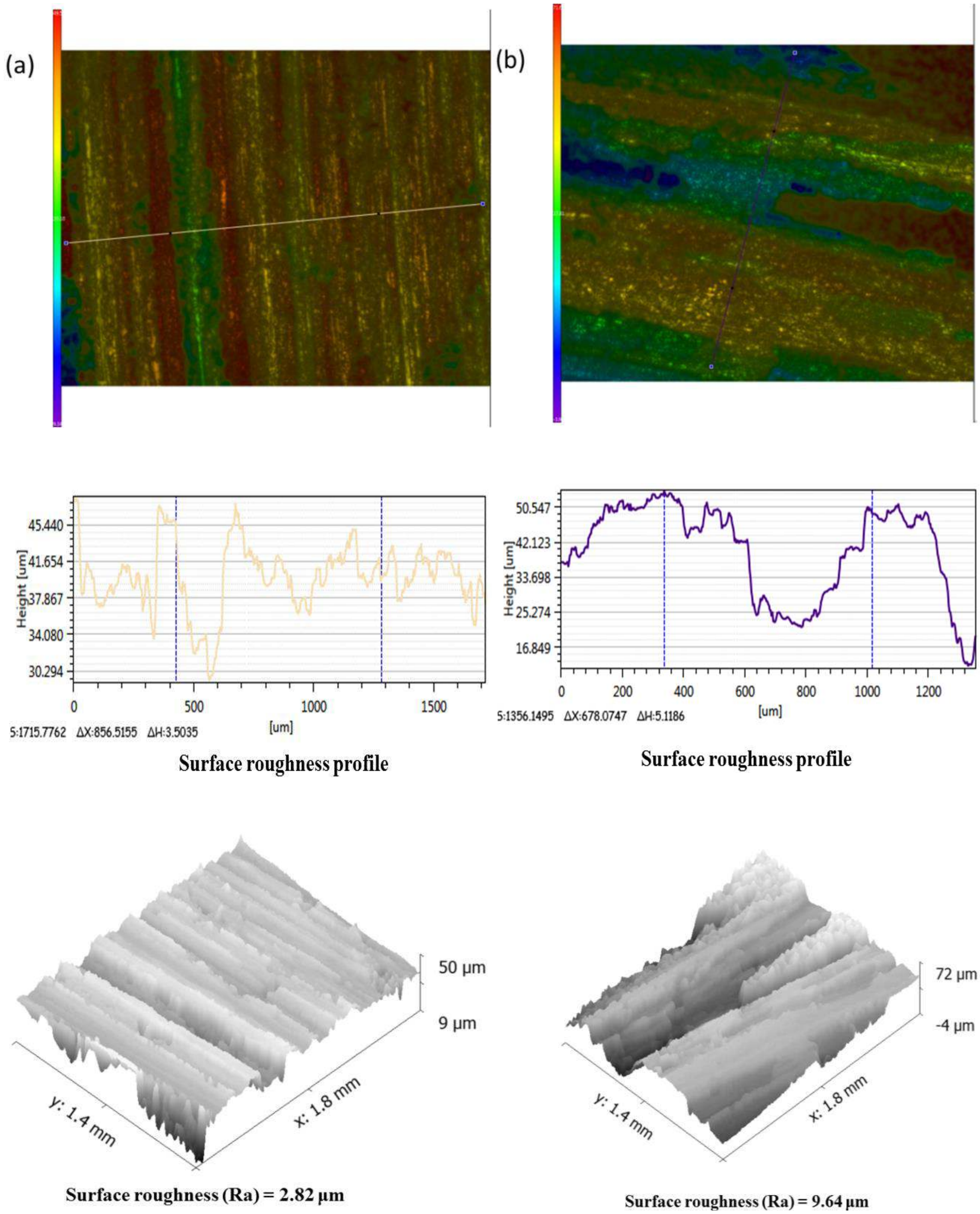

Figure 5.13 - 2D and 3D topography of worn surface of AA5052 - 6 vol. % ZrB_2 composite at (a) RT and (b) 200°C, at 20 N load and 0.5 m/s sliding velocity under profilometer [Kumar et al., 2016b]

5.4.3 Effect of Normal Load

Wear rate, wear rate per unit vol. % ZrB_2 and coefficient of friction all are affected by applied normal load as shown in Figs. 5.14, 5.15 and 5.16.

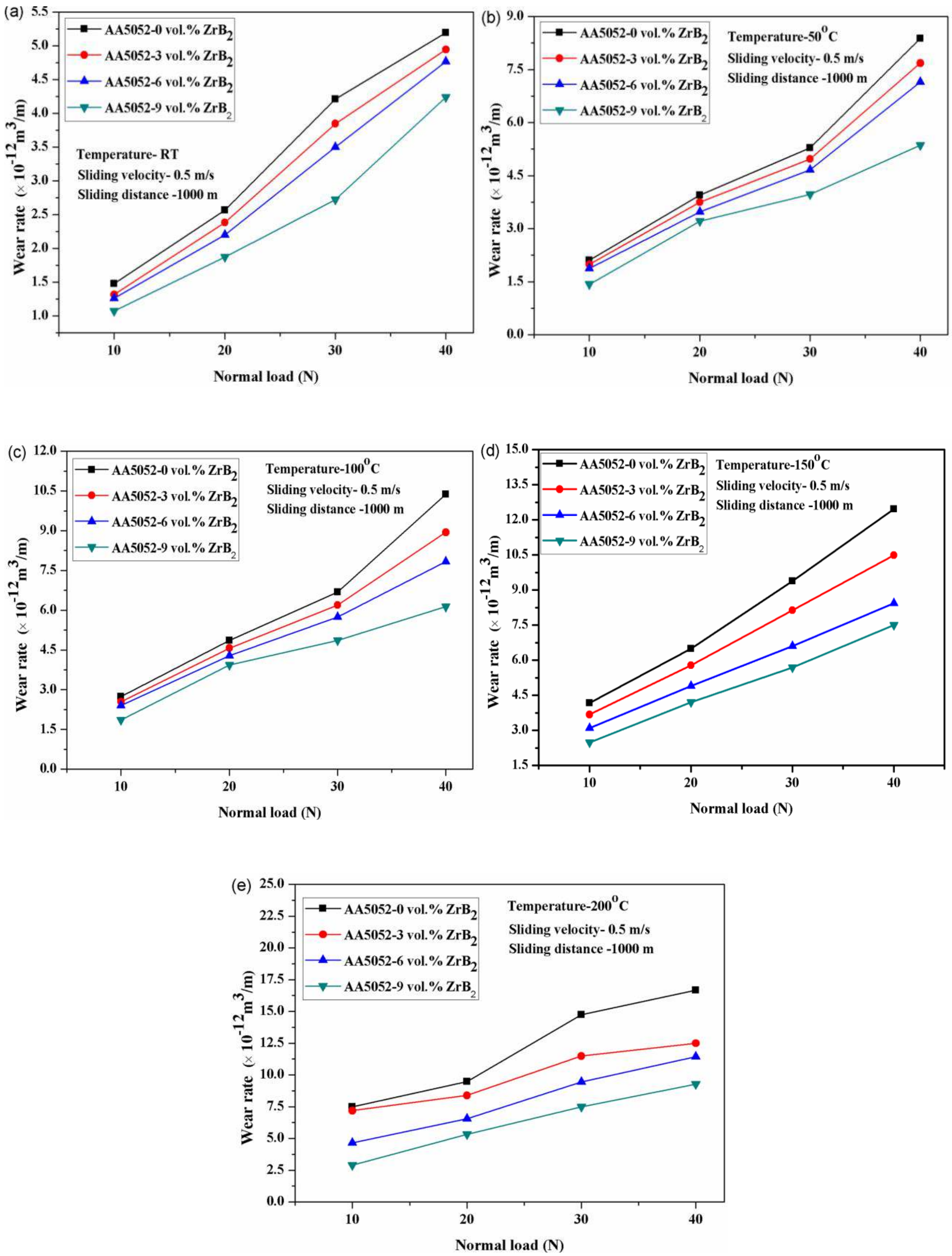

Figure 5.14 - Variation of wear rate with different loads at (a) RT (b) 50°C (c) 100°C (d) 150°C and (e) 200°C for different composites [Kumar et al., 2016b]

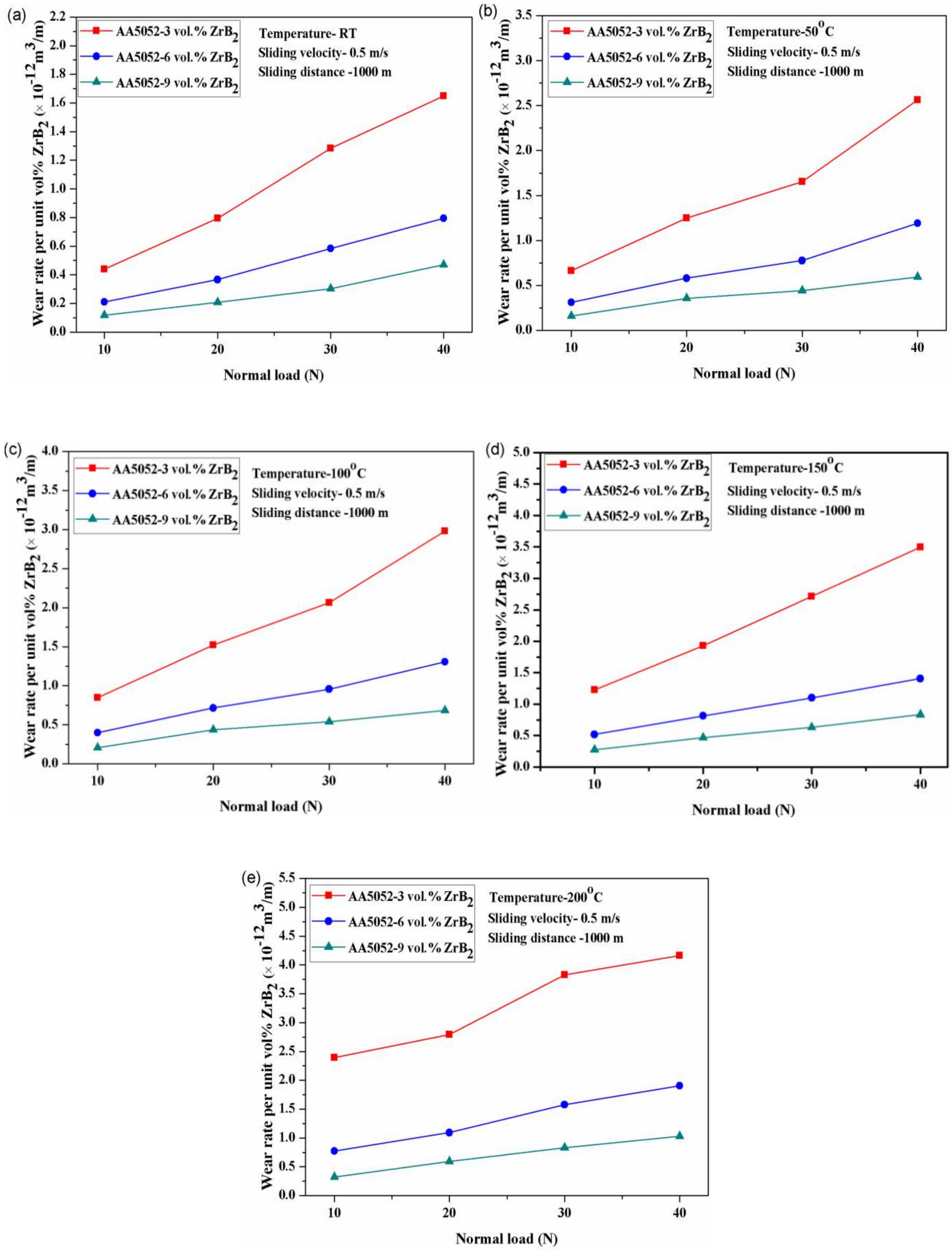

Figure 5.15 - Variation of wear rate per unit vol. % ZrB_2 with different loads at (a) RT (b) 50°C (c) 100°C (d) 150°C and (e) 200°C for different composites [Kumar et al., 2016b]

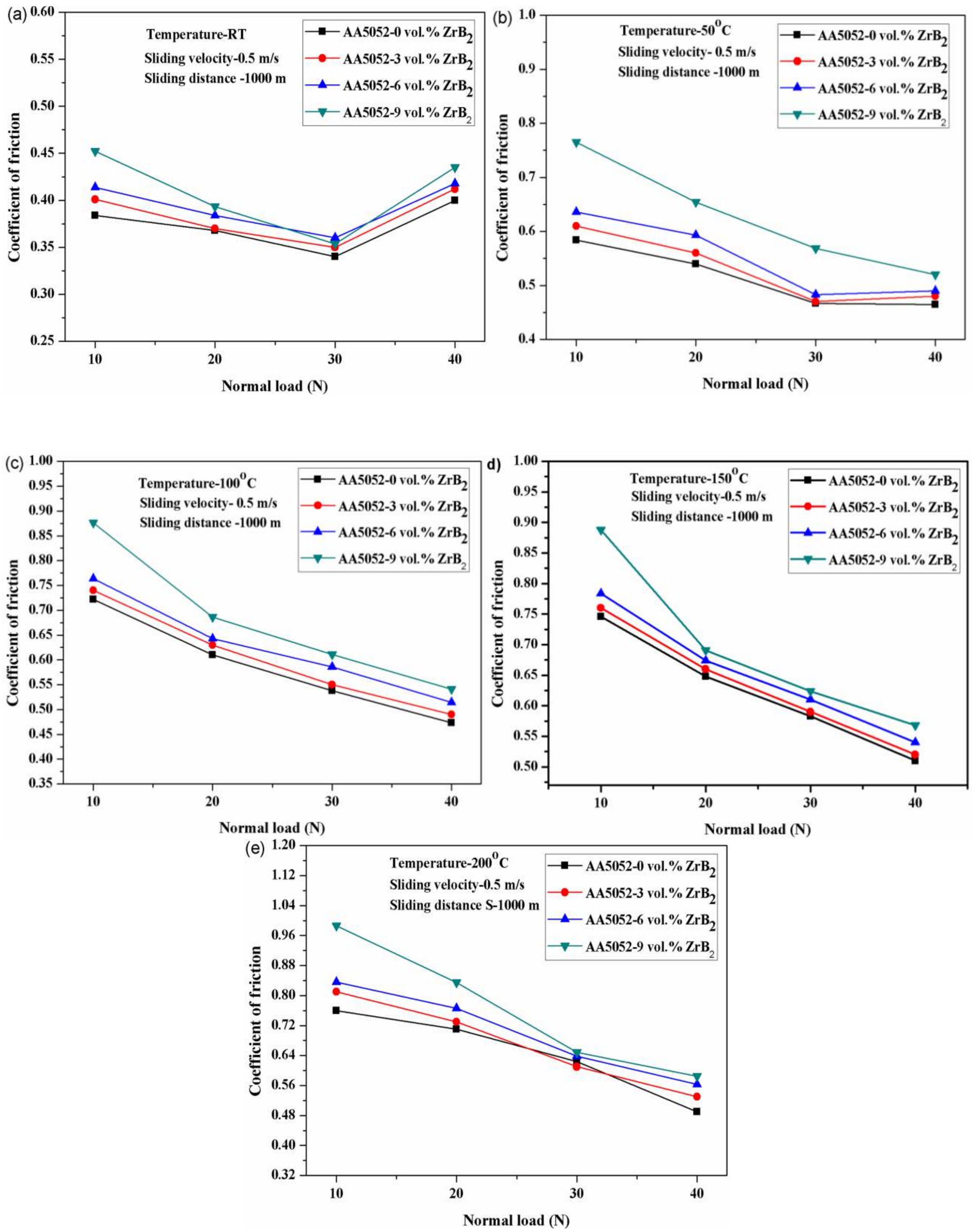

Figure 5.16 - Variation of COF with different loads at (a) RT (b) 50°C (c) 100°C (d) 150°C and (e) 200°C for different composites [Kumar et al., 2016b]

Wear rate increases linearly with increase in load (Fig. 5.14a-e) for all compositions and same phenomenon is observed at all temperatures. The increased wear rate at higher loads may be attributed to the extensive plastic deformation of the aluminium matrix and crack nucleation at the particle matrix interface leading to particle de-cohesion. Due to work hardening in the subsurface material, the cracks are nucleated around the reinforcement particles. These cracks may propagate into the matrix and eventually join together under repeated loading. As a result deformation in matrix allows the particles to come out and wear rate is increased [Demirel and Muratoglu, 2011; Tu and Liu, 1998]. However, the wear rate decreases with increase in the amount of ZrB_2 particles due to reduction in deformation of aluminium matrix. Further, lower wear rate may also attribute to the enhanced strength and hardness due to grain refinement and dispersion strengthening of the matrix [Kumar et al., 2010b]. Wear rate per unit vol. % ZrB_2 is an important parameter to interpret the wear results. This parameter gives an indirect measure of load bearing capacity of composites. It is observed from Fig. 5.15a-e that wear rate per unit vol. % ZrB_2 decreases drastically beyond 3 vol. % ZrB_2 due to high vol. % of ZrB_2 particles. At room temperature coefficient of friction decreases with increase in loads up to 30 N but beyond this load a sharp increase in coefficient of friction is observed (Fig. 5.16a), but with temperature rise coefficient of friction continuously decreases with increase in load within the range of experiment (Fig. 5.16b-e). Lower value of coefficient of friction may be attributed to the thickening of the oxide layer on the worn surface due to high working temperature with increase in applied load [Zhu et al., 2012; Kumar et al., 2016b].

Worn surface morphology of AA5052 - 9 vol. % ZrB_2 composite at 150°C is shown in Fig. 5.17a-d. Worn surface reveals smooth areas, less delamination, shallow grooves, shallow ploughing at low normal loads (Fig. 5.17a-b) which is indicative of mild-oxidative wear. Whereas, at higher load worn surface reveals large flakes, high delamination, deep grooves and large number of cracks (Fig. 5.17c-d) indicating severe-metallic wear and high wear rate is observed. 3D profilometry and surface roughness measurement of worn surface reveal increased surface roughness at 40 N load as compared to 10 N (Fig. 5.18a-b) [Kumar et al., 2016b].

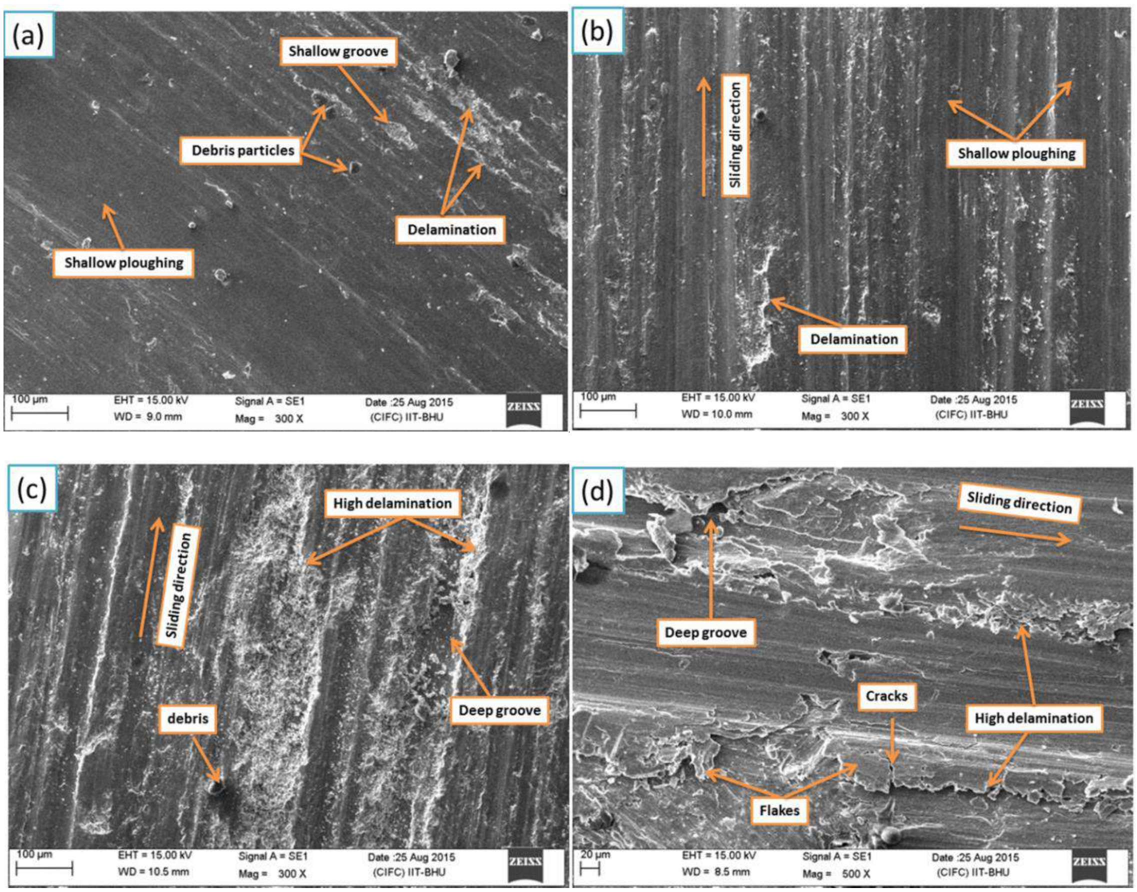

Figure 5.17 - Worn surface morphology of AA5052 - 9 vol. % ZrB_2 composite at (a) 10 N (b) 20 N (c) 30 N and (d) 40 N load, at 150°C and 0.5 m/s sliding velocity [Kumar et al., 2016b]

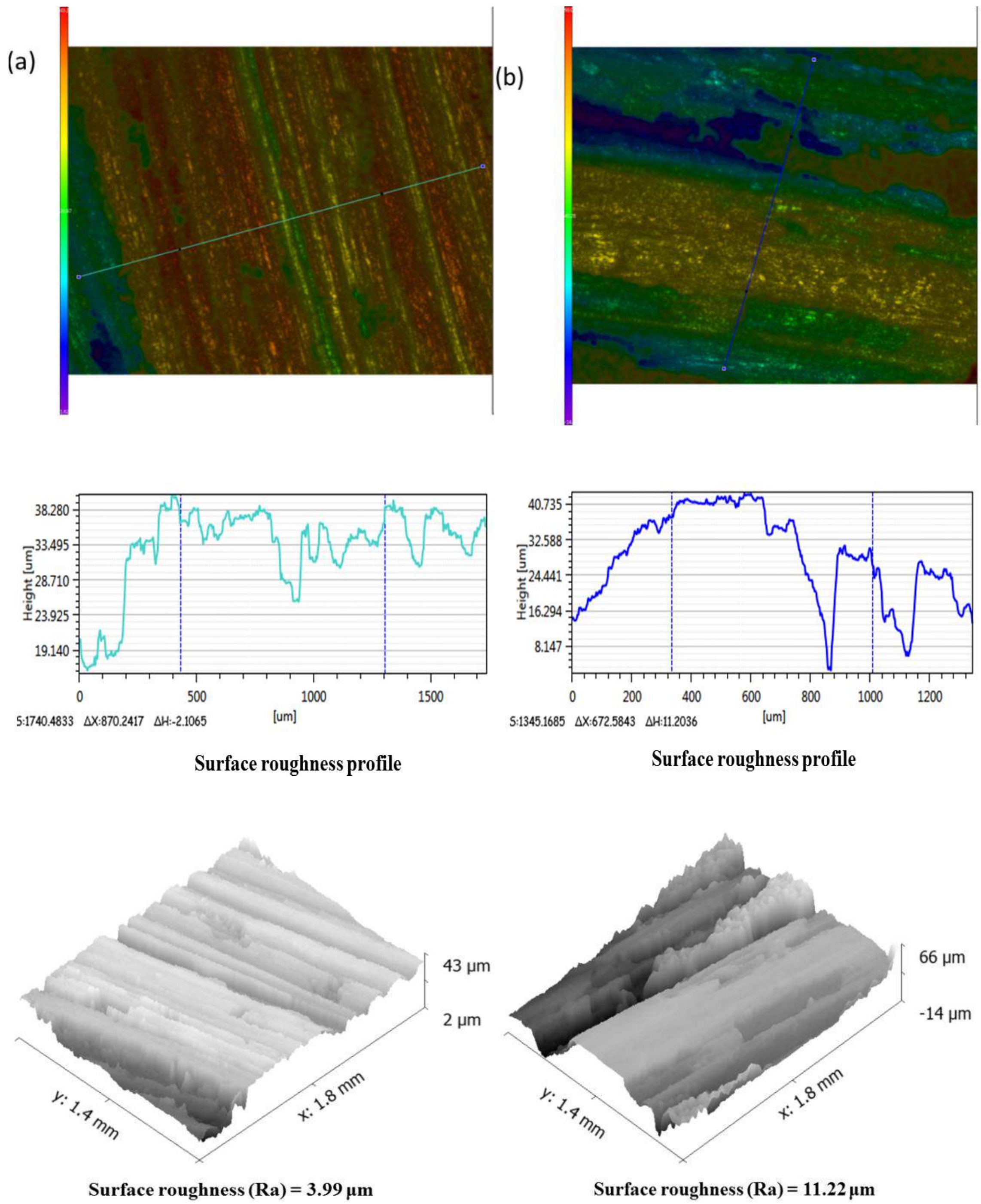

Figure 5.18 - 2D and 3D topography of worn surface of AA5052 - 9 vol. % ZrB_2 composite at (a) 10 N and (b) 40 N load, at 150°C and 0.5 m/s sliding velocity under profilometer [Kumar et al., 2016b]

5.5 Conclusions

Following conclusions are drawn from the present chapter.

1. For a constant load and temperature wear rate decreases with increase in vol. % of ZrB_2 particles, whereas, coefficient of friction shows reverse trend.
2. For a constant load and composition both wear rate and coefficient of friction increase with increase in temperature.
3. Wear rate and wear rate per unit vol. % ZrB_2 particles increase with increase in applied load at constant temperature.
4. Transition temperature of wear mode from mild-oxidative to severe-metallic shifts from 100° to 150°C with the addition of 9 vol. % ZrB_2 particles in the base alloy, which indicates that with increase in ZrB_2 reinforcement working temperature can be increased.
5. Worn surface morphology reveals reduced delamination, metal flow and shallow ploughing at higher vol. % of ZrB_2 particles and this phenomenon is observed even at high temperature.
6. Worn surface and debris analysis show mild-oxidative wear at low load and temperatures and severe-metallic wear at higher loads and temperatures. Profilometry study also reveals the increased surface roughness at high load and temperatures.
7. ZrB_2 particles widen the application range and areas of AA5052 alloy, and even suitable for high temperature applications.